Modeling of Highly-Nonlinear HBT Characteristics using a Distributed Thermal Subcircuit Derived from Pulsed Measurements

Shawn S.H. Hsu, Donald Sawdai, and Dimitris Pavlidis

Department of Electrical Engineering and Computer Science
The University of Michigan, 1301 Beal Ave.
Ann Arbor, MI 48109-2122

Abstract

The nonlinear DC and RF properties of HBTs were modeled using a customized *Gummel-Poon*-based large signal model. The characterization and modeling techniques presented here were validated using PNP InP-based HBTs, which manifest highly nonlinear features. On-wafer pulsed DC measurements were performed on these HBTs in order to extract various second-order effects. These pulsed measurements indicated the presence of distributed thermal resistances and thermal capacitances. An analytical parameter extraction procedure was then used to extract model data from measured small-signal *S*-parameters and from the DC characteristics. Pulsed characteristics under different pulse widths and different substrate temperatures were employed to complete the model extraction. Good agreement was obtained between the modeled and measured DC, pulsed, small-signal, and large-signal microwave characteristics. The approach developed in this work is useful for modeling of highly nonlinear HBT characteristics, and it is directly applicable to the HBT power amplifiers often encountered in wireless communication circuits and systems.

I. Introduction

Significant effort has been put forth to develop large-signal models for NPN HBTs, and a variety of approaches have been used to model thermal effects [1, 2]. However, accurate modeling of the highly nonlinear properties encountered in HBTs is still an issue. This paper addresses an approach suitable for modeling such characteristics. The device selected for this purpose is an InP-based PNP HBT. The presented approach is, however, more general and applicable to all HBT types. GaAs-based PNP HBTs have been reported with record performance, making possible complementary HBT circuits for power applications [3]. InP-based PNP devices were also employed together with NPN HBTs in order to demonstrate the feasibility of PNP-NPN push-pull amplifiers [4]. Therefore, the development of a large-signal model suitable for PNP HBTs offers the possibility of validating the described modeling approach while at the same time being of practical importance for wireless circuits and systems that often employ such components.

The InAlAs/InGaAs PNP HBTs used in this study were fabricated in-house and demonstrated 26 GHz f_{max} and 0.49 mW/μm^2 maximum output power. The HBTs showed various second-order non-ideal characteristics such as *self-heating*, the *Early effect*, and the *Kirk effect*. Drift-diffusion simulation suggests that PNP HBTs show more pronounced second-order effects than NPN HBTs due to the lower hole-mobility [5]. They are therefore excellent devices to validate the reported modeling approach. Note that individual evaluation of the non-ideal effects present in the device is essential to obtain an accurate large-signal model.

In this study, pulsed measurements with different pulse widths and device substrate temperatures proved to be a powerful tool for separating various non-linear effects present in the HBTs in order to generate an accurate large-signal RF model. First, the isothermal characteristics were modeled to accurately evaluate the thermally independent parameters. A thermal subcircuit with two resistances and two capacitances was then included to model the device thermal characteristics. Then, the microwave parameters were extracted from the small-signal *S*-parameters under "on" and "off" conditions, and further optimization with fixed DC parameters was performed to achieve a consistent model under various biases and frequencies. The described approach allows extraction and modeling of various second-order effects of the devices by combing DC, pulsed, small-signal microwave, and large-signal microwave measurements.

The pulsed characterization described in this work turns out to play a predominant role in modeling non-linear device properties.

II. Pulsed Characterization and Non-linear Parameter Extraction

Pulsed measurements were performed using two synchronized pulse sources and an inductively-coupled current probe. A single pulse with 200 ns width (period $T = \infty$) was used for each data point to ensure that thermal effects were not accumulated during the measurements. *Figure 1* shows the DC (room temperature) and pulsed measurement results. As can be seen, the *Early voltage* V_a can be easily extracted from the nonzero slope of the pulsed I_c-V_{ec} characteristics in the active region. In addition, the reduced current gain caused by the *Kirk effect* (rapid widening of the charge-neutral base region when the collector current density J_C exceeds the critical value J_k) can be distinguished from the thermal effects by examining the pulsed results. Normally, both thermal effects and the *Kirk effect* result in decreased gain at high current levels. Therefore, their individual impacts cannot be separated by examining only the DC characteristics. The use of pulsed measurements in this work allowed separation of thermal and *Kirk* effects, which permitted physical modeling of both non-linearities.

The thermal model was derived for the HBTs by measuring the device under different substrate temperatures and pulse widths. As shown in *Figure 2*, transient measurements using a single long pulse (50 μs) indicate that the collector current reduces rapidly within 1μs and then slowly approaches a value corresponding to the DC operation. Two *RC* time constants can be extracted by fitting these two regions of the I_c *vs. t* measurements to exponential decays of the form $I_0 \cdot exp(- t/RC)$. By further comparing the current gain at different substrate temperatures (30°C, 50°C, 70°C) using pulsed measurements at the same base current, the total thermal resistance $R_1 + R_2$ can be extracted. This extraction assumed that the current gain decreases linearly as the temperature increases [6]. R_2 can then be extracted from the difference in current gain between short and long pulses (200 ns and 1 μs) at room temperature. The performed study suggests that a distributed thermal subcircuit including two different thermal resistances and two thermal capacitances is appropriate for describing the device characteristics. The incorporation of such a subcircuit in the nonlinear device model is critical for accurate reproduction of the pulsed characteristics.

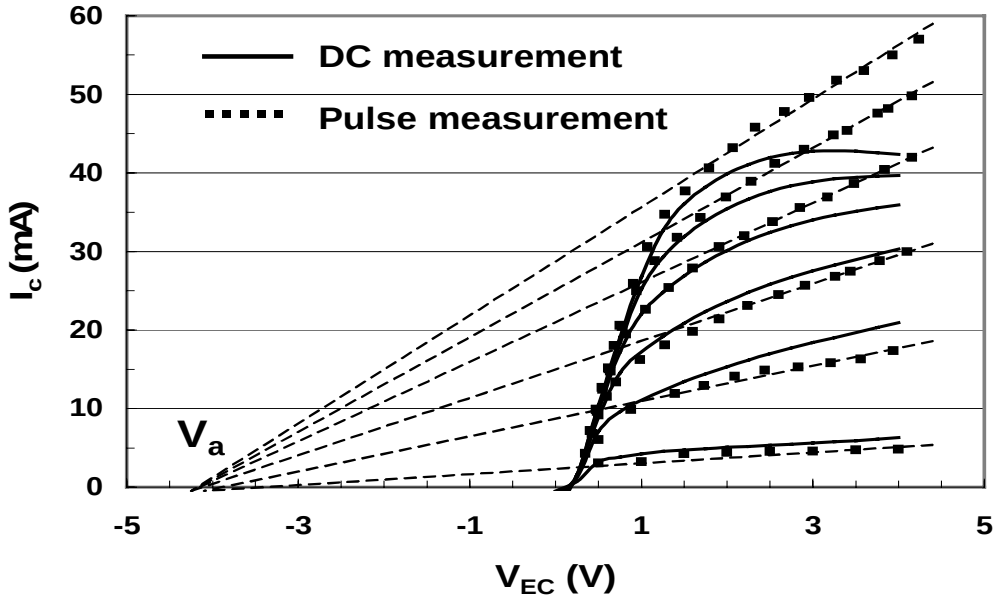

Figure 1. *DC and pulsed measurement results for 5×10 μm² PNP HBT I_c-V_{ec} characteristics (I_b= 0.5mA/ step). V_a is the Early voltage.*

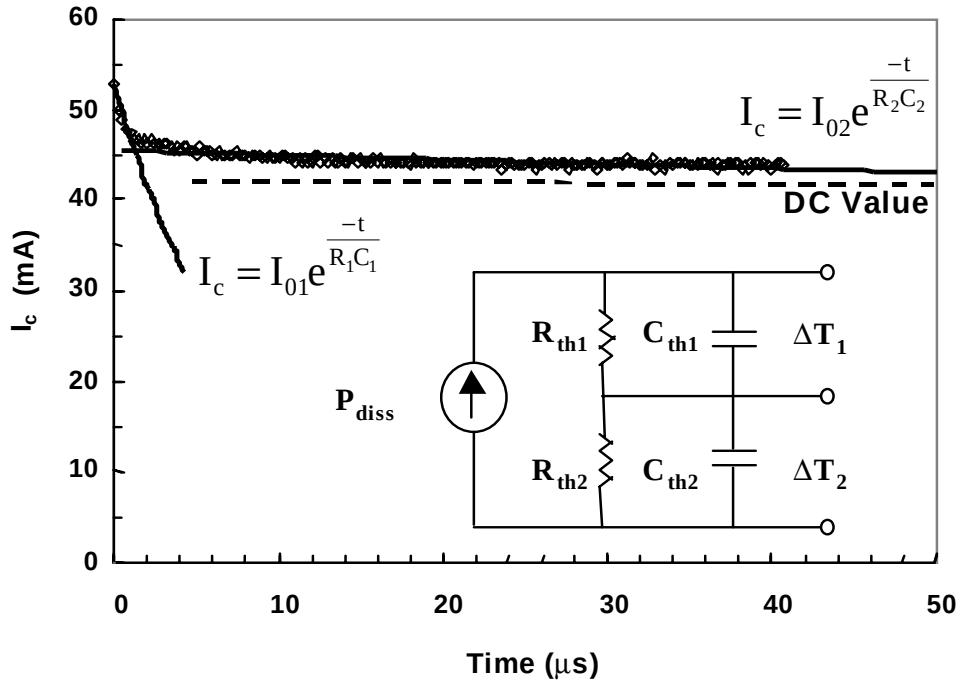

Figure 2. *Pulsed measurement I_c transient characteristics (I_b= 3.0 mA, V_{ec}= 3 V) for 5×10 μm^2 PNP HBT. The data allows extraction of a distributed thermal subcircuit.*

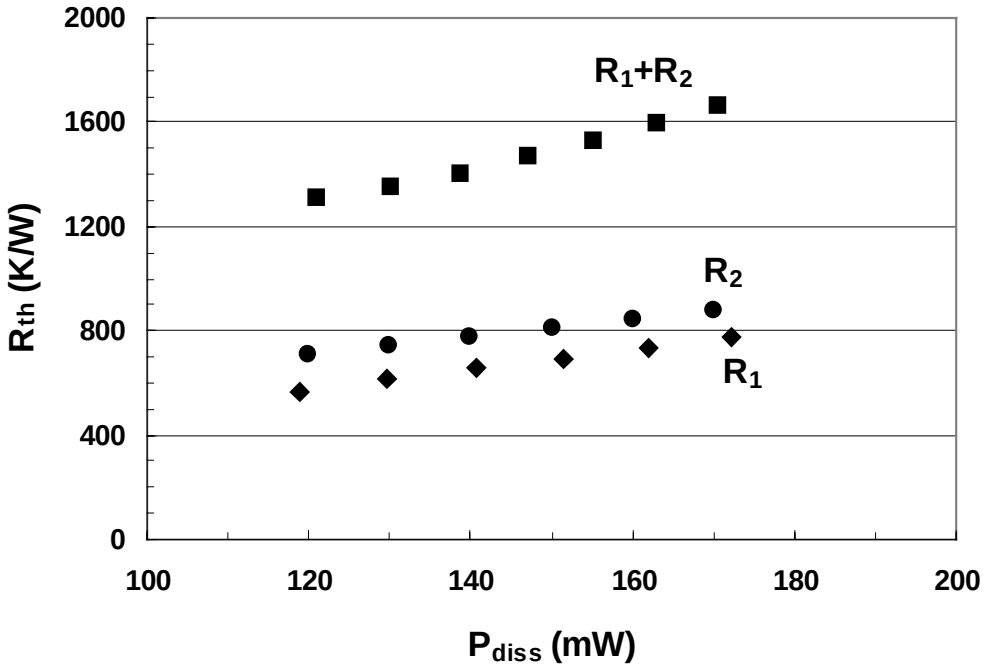

Figure 3*. Measured thermal resistances at a constant base current (I_b= 3mA).*

The measured thermal resistances are shown in *Figure 3*. Physically, R_1 represents the thermal resistance from the E-B junction to the top of the substrate, and R_2 represents the thermal resistance between the front and back sides of the substrate. By assuming that the device is a point heat source on the InP substrate (thermal conductivity = 0.68 W/K-cm) and by using the actual collector area (25×30 μm^2) and substrate thickness (350 μm), the thermal resistance R_2 was estimated to be 782.3 K/W using the analytical formula from [7]. This calculated R_2 is in very good agreement with the measurement result of R_2 = 710 K/W at P_{diss} = 120 mW. Note that the measurement results indicated an increase of R_{th} with power dissipation P_{diss} due to the decreased thermal conductivity of InP at higher temperatures. Therefore, both thermal resistances R_1 and R_2 were modeled as linear functions of dissipated power in the thermal subcircuit. The thermal capacitances C_1 and C_2 can be estimated from the measured thermal time constants R_1C_1 and R_2C_2 once the values of R_1 and R_2 have been obtained. The results indicated that C_2 (~ 0.1 μF) is significantly larger than C_1 (~ 0.4 nF), which agrees with the relative sizes of the substrate (C_2) and the HBT (C_1).

III. Large-Signal Modeling Procedure and Verification

This section describes our large-signal modeling procedure step by step. First, small-signal *S*-parameter data was used to analytically extract bias-independent parasitic resistances through an impedance block conditioned optimization procedure [8]. Parasitic resistance values such as R_e, R_{ci}, R_{cx}, R_{bi}, and R_{bx} extracted from high frequency *S*-parameters were found to be most representative of the device properties and allowed therefore better modeling than DC extraction of these parameters. Second, the junction diode (both B-E and C-B junctions) ideality factors and saturation current were then extracted from forward and reverse DC *Gummel plots*. In addition, the *Early Effect* was modeled so that the saturation current and forward current gain are both proportional to ($1 - V_{cb}/V_a$), where V_a is the *Early Voltage*. The *Kirk effect* was then added to the model by using an empirical factor $A\cdot\exp(-V_{eb}/BkT)$ multiplied with the E-B junction saturation current I_s, where *A* and *B* are fitting parameters and *k* is *Boltzmann's* constant. The modeled I_c-V_{ec} characteristics were compared to the pulsed characteristics to ensure the accuracy of the isothermal model up to this step. The thermal subcircuit was then included in the model to achieve the complete nonlinear DC model. The junction temperature difference ΔT arising from the power P_{diss} dissipated in the HBT can be calculated from the voltage drop across the thermal resistances, and the current gain was modeled as a function of this ΔT self-consistently. *Figure 4* demonstrates good agreement between the modeled and measured DC I_c-V_{ec} characteristics. *Figure 5* shows the low-frequency transient characteristics calculated from the full HBT model (including thermal capacitances but excluding RF junction and diffusion capacitances) at I_b= 3mA and V_{ec}= 3V, which demonstrates very good agreement with the measured data.

In order to complete the RF model, the parasitic inductances (L_e, L_c, and L_b), junction depletion capacitances (C_{be} and C_{bc}), and parasitic pad capacitances were extracted from the "off" state *S*-parameters as described in the previous section. The microwave equivalent-circuit parameters under active bias conditions were extracted from small-signal *S*-parameters measured in the HBT "on" state. Parameters obtained from the device "on" state, such as the bias-dependent junction diffusion capacitances and the base and collector transit times, were used as initial values for large-signal model optimization. Finally, the large-signal model was completed by using optimized semi-empirical junction capacitance equations [9] in order to improve the model fit to the measured small-signal *S*-parameters while maintaining the excellent fit to the DC characteristics. This hybrid extraction approach employing high-frequency and DC data was found best for modeling the HBTs.

To verify our model under large-signal operation, the modeled and measured microwave power performance was compared. On-wafer power characterization was performed at 10 GHz using a load-pull system with electromechanical tuners for control of the input and output impedances. The HBT was biased at V_{ec}= 4.0 V and I_c= 12.6 mA, and Γ_L and Γ_S were optimized for maximum power gain. The power performance was then calculated using the large-signal model at the same bias and tuner reflection coefficients as in the experimental measurements. *Figure 6* shows the calculated and measured results for P_{out}, Gain, and PAE. Very good agreement was obtained over a wide range of input power levels.

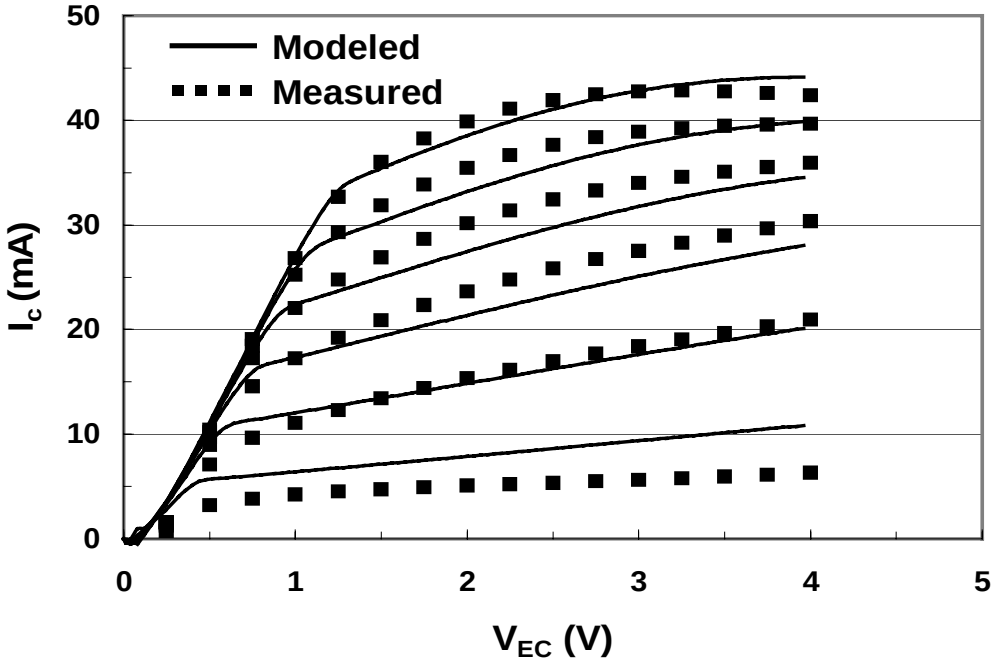

Figure 4. *Measured and modeled HBT DC I_c-V_{ec} characteristics for 5×10 μm^2 PNP (I_b= 0.5mA/ step).*

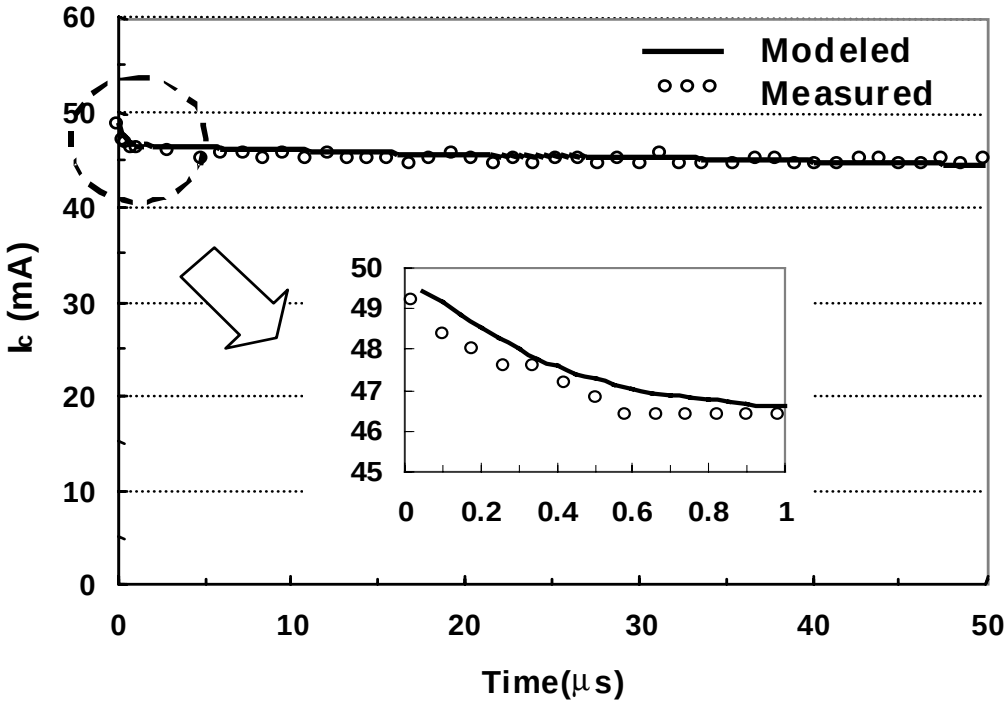

Figure 5*. Measured and modeled pulsed transient for 5×10 μm^2 PNP HBT (I_b= 3.0 mA, V_{ec}= 3 V).*

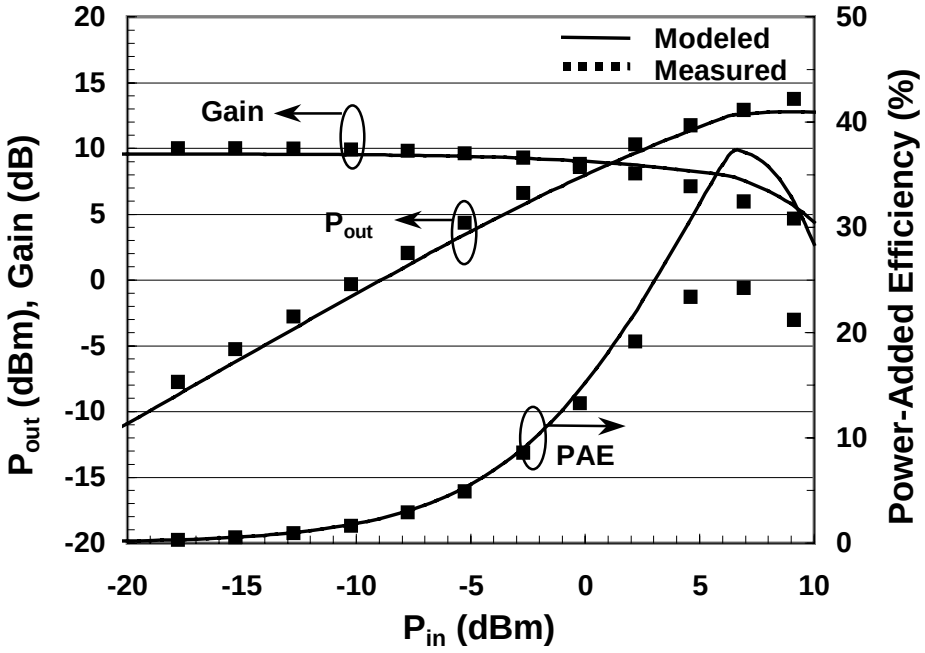

Figure 6*. Measured and modeled results for 5×10 μm^2 PNP HBT power characteristics at 10 GHz.*

IV. Conclusion

The large-signal characteristics of InP-based PNP HBTs were measured, characterized, and modeled. Pulsed measurements indicated that a distributed two-resistance two-capacitance thermal subcircuit accurately reflects the self-heating of the HBT. The systematic approach developed here modeled the HBTs with very high accuracy despite the highly nonlinear characteristics of the devices. The results demonstrate that the presented model and extraction procedures are appropriate for accurate modeling of the DC, and high-frequency small-signal and large-signal microwave properties of HBTs with high non-linearity as necessary for microwave circuit design.

[References]

[1] A. Samelis, and D. Pavlidis, "Analysis of the Large-Signal Characteristics of Power Heterojunction Bipolar Transistors Exhibiting Self-Heating Effects," *IEEE Trans. Microwave Theory and Tech.* vol. 45, no. 4, pp534-542, Apr. 1997.

[2] K. Lu, P. A. Perry, and T. J. Brazil, "A New large-signal AlGaAs/GaAs HBT Model Including Self-Heating Effects, with Corresponding Parameter-Extraction Procedure," *IEEE Trans. Microwave Theory and Tech.* vol. 43, no. 7, pp1433-1445, Jun. 1997.

[3] D. G. Hill, H. Q. Tserng, and T.S. Kim, "65/90 GHz Complementary HBT Technology," *Electronics Letters*, vol. 30, no. 7, pp597-598, Mar. 31 1994.

[4] D. Sawdai, and D. Pavlidis, "InP-based Complementary HBT Amplifiers for Use in Communication Systems," *Topical workshop on Heterostructure Microelectronics for Information Systems Applications*, Kanagawa, Japan, Aug. 30-Sep. 2, 1998.

[5] D. Sawdai, X. Zhang, D. Pavlidis, and P. Bhattacharya, "Performance Optimization of PNP InAlAs/InGaAs HBTs," *IEEE Cornell Conf. on Advanced Concepts in High Speed Semiconductor Devices and Circuits*, Ithaca, NY. 1997, pp269-277.

[6] D.E. Dawson, A. K. Gupta, and M. L. Salib, "CW Measurement of HBT Thermal Resistance," *IEEE Trans. Electron Devices*, Vol. 39, pp.2235-2239, Oct. 1992.

[7] K. Ikossi-Anastasiou, N. Valsaraj, and R. Sabbah, “Pulsed Measurements on InAlAs/InGaAs HBTs with Enhanced Performance,” *IEEE Cornell Conf. on Advanced Concepts in High Speed Semiconductor Devices and Circuits*, Ithaca, NY. 1997, pp. 287-296.
[8] A. Samelis, and D. Pavlidis, “DC to High-frequency HBT-Model Parameter Evaluation Using Impedance Block Conditioned Optimization,” *IEEE Trans. Microwave Theory and Tech.* vol. 45, no. 6, pp886-897, Jun. 1997.
[9] R. Hajji, A. Kouki, S. El-Rabaie, and F. Ghannouchi, “Systematic DC/Small-Signal/Large-Signalanalysis of Heterojunction Bipolar Transistors using a New consistent Nonlinear Model,” *IEEE Trans. Microwave Theory and Tech.* vol. 44, no. 2, pp233-241, Feb. 1996.

Work supported by ARO-MURI (DAAH04-96-1-0001)